

# Removal of chlorobenzene and 1,4-dichlorobenzene using novel poly-o-toluidine zirconium(IV) phosphotellurite exchanger<sup>☆</sup>



Aparna Mohan<sup>\*</sup>, Nimisha K.V., Janardanan C.

PG and Research Department of Chemistry, Sree Narayana College, Kannur, Kerala 670007, India

## ARTICLE INFO

### Article history:

Received 29 June 2016

Accepted 8 February 2017

Available online 7 March 2017

### Keywords:

Poly-o-toluidine

Composite exchanger

Chlorobenzene

Dichlorobenzene

Adsorption

## ABSTRACT

Novel hybrid exchanger poly-o-toluidine zirconium(IV) phosphotellurite was synthesized and physico-chemical properties of the material were well studied by FTIR, XRD, TGA, SEM-EDX and TEM analysis. The composite exchanger showed good ion exchange capacity and excellent removal potential towards US Environmental Protection Agency listed priority pollutants like chlorobenzene and 1,4-dichlorobenzene. The factors affecting the adsorption like time, pH and temperature were studied in detail using UV spectrophotometry. More than 90% of the pollutants were successfully removed using the exchanger. The composite also showed selectivity towards heavy metal ions, especially mercury ions. The sorption kinetics of the material was studied in detail using pseudo first order and pseudo second order kinetics. The material followed pseudo second order kinetic model indicating chemisorption of the pollutants. The composite can be successfully used for environmental remediation purposes.

© 2017 Published by Elsevier B.V. on behalf of Tomsk Polytechnic University.

This is an open access article under the CC BY-NC-ND license.

(<http://creativecommons.org/licenses/by-nc-nd/4.0/>)

## 1. Introduction

Water is the basic necessity for life but the quality and availability of potable water is decreasing drastically. Water bodies are seriously contaminated by various factors such as heavy metals, noxious chemicals, pesticides and fertilizers, radioactive wastes etc. which are intentionally or unintentionally discharged into it from diverse sources. Adsorption, ion exchange, oxidation, filtration, chemical precipitation, membrane separation, solvent extraction, electro dialysis etc are the various methods adopted for water treatment and purification [1–5]. Among the various pollutants that contaminate water bodies, priority pollutants are a class of compounds of extreme concern. The US Environmental Protection Agency (EPA) has listed 126 pollutants as priority pollutants which include both heavy metals and specific organic compounds. Compounds are categorized under priority pollutants on the basis of their toxicity, degradability, persistence and effect on organisms. This class of pollutants is mainly found in water bodies and pos-

sesses high toxicity; hence removal of priority pollutants from water bodies is absolutely relevant [6].

Ion exchange is a simple, attractive and widely used method which has well established its significance in separation science and metal ion recovery. The latest advance in this field is the composite exchangers. Composite exchangers are new class of materials which gained appreciable acceptance by overcoming the major drawbacks of inorganic and organic exchangers. They are materials containing an organic matrix and an inorganic moiety [7]. Applications of composite exchangers include water purification, separation of metal ions, radioactive waste removal, development of fuel cells, ion selective membrane electrodes, catalysis etc [8–10]. Innumerable works has been carried out using newly synthesized composite exchangers and the major application of composite exchangers is their environmental remediation capacity [11]. They are widely used for their ion exchange property and adsorption capacity towards various kind of pollutants. Though water purification has been extensively carried out using composite exchangers, elimination of priority pollutants using composite materials has not been studied much [12]. Only negligible works have been carried out in this area and considering this factor, the newly synthesized exchanger was made used for the removal of priority pollutants.

The hybrid exchanger was studied for its capability to adsorb priority pollutants such as chlorobenzene, 1,4-dichlorobenzene and

<sup>☆</sup> Peer review under responsibility of Tomsk Polytechnic University.

<sup>\*</sup> Corresponding author. Department of Chemistry, Sree Narayana College, Kannur, Kerala, India. Tel: +919633161746; fax: +919633161746.

E-mail address: [aparnakaryat@gmail.com](mailto:aparnakaryat@gmail.com) (A. Mohan).

mercury ions. Chlorobenzene (CB) and 1,4-dichlorobenzene (DCB) are highly toxic organic compounds and are ranked 7th and 27th in the priority pollutants list. Mercury on other hand is the 10th priority pollutant among the heavy metals [6]. Chlorobenzene is a colorless, flammable liquid widely used in the manufacture of several chemicals such phenol, aniline, nitrochlorobenzene, triphenylphosphene, thiophenol etc. It is primarily used as solvent for paints, resins and is an intermediate in the synthesis of insecticide such as DDT and dyes. Pulp and paper industries, leather tanning industries and chemical industries are the major industries releasing chlorobenzene containing effluents. Inhalation or exposure to CB may cause numbness, muscular spasm and lethal effect on central nervous system. 1,4-dichlorobenzene is mainly used as fumigant for the control of moths. It is also used as intermediate for synthesis of dyes, pharmaceuticals, plastics and various other chemicals. They are highly carcinogenic in nature and its toxicity includes mild effects such as headache, nausea, dizziness etc to acute health effects such as damage of liver, kidney, central nervous system etc. Mercury enters water bodies mainly from dental amalgam, thermometer factories, refineries etc. Methyl mercury is the prime organic mercury compound which can enter into food chain and results in biomagnification. It mainly damages the nervous system and is carcinogenic. Elemental mercury is also poisonous since it leads to brain and kidney damage, insomnia, memory loss etc.

Literature review suggests that only few studies have been carried out for the removal and adsorption of chlorobenzene and 1,4-dichlorobenzene. Adsorption of CB using activated carbon has been discussed and the adsorption kinetics has been detailed [13,14]. In another study, carbon nanotubes and graphene has been used for the adsorption of chlorobenzene [15]. Use of other adsorbents such as marine sediments [16]  $\gamma$ - $\text{Al}_2\text{O}_3$  has also been reported for the removal of CB [17]. The degradation of 1,4-dichlorobenzene in acetonitrile-water solution has been investigated and reported by Qi Liu et al. [18]. The present study focuses on the synthesis and characterization of novel composite exchanger poly-o-toluidine zirconium(IV) phosphotellurite (POT ZrPTe) and its efficacy in removing priority pollutants from aqueous system. Effect of various parameters that affect the adsorption and the kinetic aspects of removal of the CB and DCB using the proposed composite exchanger has also been studied and discussed.

## 2. Materials and methods

### 2.1. Chemicals and reagents

The main chemicals used were Zirconium oxychloride (E. Merck), Sodium tellurite (E. Merck), Sodium orthophosphate (Loba Chemie, India), O-toluidine (Loba Chemie, India), Chlorobenzene (Loba Chemie, India) and 1,4-dichlorobenzene (Loba Chemie, India). All other reagents and chemicals used for the synthesis were of analytical grade. Double distilled water was used throughout the synthesis process.

### 2.2. Instrumentation

For IR studies, FTIR spectrometer model IR Tracer-100, Shimadzu was used. X-ray diffractometer Rigaku Rint TTR-III for X-ray diffraction studies and Shimadzu DTG-60H was used for thermogravimetric analysis. SEM images were taken using Jeol JSM-7500F and UV-Visible spectrophotometer model JASCO V660 was used for spectrophotometric measurements. The transmission electron mi-

crographs (TEM) of the sample was acquired using a JEOL/JEM-3200FS.

### 2.3. Synthesis of composite exchanger

#### 2.3.1. Synthesis of poly-o-toluidine

Simple oxidative polymerization technique was used for the polymerization of o-toluidine. 0.4M ammonium persulfate prepared in 4.0M HCl was continuously added to 10% o-toluidine prepared in 2.0M HCl with stirring using a magnetic stirrer for 2 hours at 0 C till a dark green colored gel was obtained. The gel obtained was kept for 24 hours at 0 C [19].

#### 2.3.2. Synthesis of zirconium(IV) phosphotellurite

For the synthesis of inorganic part zirconium(IV) phosphotellurite, 0.05M solution of sodium orthophosphate and sodium tellurite were mixed vigorously by constant stirring maintaining the pH in acidic range. The clear solution formed was then added to 0.05M aqueous solution of zirconium oxychloride until a white gelatinous precipitate was formed. The slurry was kept for digestion for 24 hours at room temperature.

#### 2.3.3. Synthesis of poly-o-toluidine zirconium(IV) phosphotellurite composite (POT ZrPTe)

The ex-situ polymerized gels of poly-o-toluidine were added to the white gelatinous inorganic precipitate of zirconium(IV) phosphotellurite carefully with constant stirring at room temperature until a green colored thick slurry was formed. The slurry was then kept for digestion at room temperature. The gel was filtered and the excess acid was removed by continuous washing with demineralized water (DMW). The filtered out material was dried in an air oven at 30 C. After drying, the material was converted to  $\text{H}^+$  form by keeping it in 1.0M  $\text{HNO}_3$  solution for 24 hours with occasional shaking, intermittently replacing the supernatant liquid with fresh acid. The excess acid was again removed using DMW and then dried at 30 C and kept in desiccator.

### 2.4. Ion exchange capacity (IEC)

Column method was used for the determination of ion exchange capacity [20]. A glass column of 1.1 cm diameter plugged with cotton wool at the bottom was taken, to which 1g of the material in  $\text{H}^+$  form was added. 100 mL of 1.0M NaCl solution was poured to it in order to elute the  $\text{H}^+$  ions from the exchanger, maintaining the flow rate at  $1 \text{ mL min}^{-1}$ . The  $\text{H}^+$  ion content in the effluent was then determined by titrating it against a standard solution of 0.05M NaOH solution. From the titre value, the ion exchange capacity in  $\text{meq g}^{-1}$  was calculated using the relation,

$$\text{IEC} = av/w$$

where a and v are the molarity and volume of NaOH used during titration and w is the weight of the exchanger taken [20].

### 2.5. Distribution studies

Distribution coefficient,  $K_d$  is defined as the ratio of the concentration of a metal ion in the exchanger and in the solution [20]. Distribution coefficient of the composite exchanger for various metal ions in DMW was studied by batch method [21]. For this, 0.1 g of the exchanger was equilibrated with 20 mL of the metal ion solutions for 24 hours at room temperature. The metal ion concentration before and after sorption were determined by complexometric titration against standard EDTA solution. In the complexometric method, the  $K_d$  values were calculated using the formula,

$$K_d = \frac{(I - F)}{F} \times \frac{V}{W}$$

where, I and F are the initial and final volume of EDTA used, V is the volume of the metal ion solution (mL) and W is the weight of the exchanger taken [20].

### 2.6. Binary separation

To carry out quantitative separation of metal ions, 1g of exchanger packed in glass column was thoroughly washed with DMW and the mixture of two metal ions was poured into it. After loading the metal ions on to the column, they were eluted using suitable solvents. The flow rate was maintained at constant level throughout the elution process. The effluents were then titrated with standard EDTA solution.

### 2.7. Pollutant adsorption studies

Batch method was followed for carrying out the adsorption study [22]. 20 mL of 50 ppm solutions of chlorobenzene and 1,4-dichlorobenzene were shaken with known amounts of POT ZrPTE in a rotary incubator until equilibrium time was reached. After attaining the equilibrium time, the supernatant solution was analyzed spectrophotometrically to find out the residual concentration of the pollutants in the solution. The temperature dependence was studied by shaking known amount of POT ZrPTE with 20 mL of 50 ppm solutions of pollutants at room temperature and at elevated temperature. Effect of pH was also studied by following the same procedure along with varying the pH of the solution from 2 to 12. The change in concentration was calculated spectrophotometrically by measuring the  $\lambda_{\max}$  at 262 nm for chlorobenzene and 272 nm for 1,4-dichlorobenzene respectively [23].

### 2.8. Kinetic studies

For evaluating the kinetic parameters, 20 mL of 50 ppm solutions of CB and DCB were treated with 0.2g of POT ZrPTE in stoppered conical flasks at room temperature for different time intervals, maintaining neutral pH. The supernatant liquid was analyzed at definite time intervals so as to study the concentration variation.

## 3. Results and discussion

### 3.1. Synthesis, nature, stability and ion exchange capacity

The composite cation exchanger poly-o-toluidine zirconium(IV) phosphotellurite was synthesized by mixing different volume ratios of the reagents at specific pH and temperature (Table 1). From

Table 1 it is clear that the inorganic counterpart sample ZrPTE-4 showed maximum ion exchange capacity and hence that volume ratio was chosen for the synthesis of composite exchanger. Polymerization of o-toluidine was carried out by oxidation using ammonium persulfate in acidic medium (Scheme 1). To the dark green colored gels of poly-o-toluidine formed, the inorganic counterpart ZrPTE was added and mixed thoroughly to obtain the composite exchanger (Scheme 2). The composite exchanger POT ZrPTE exhibited black shining crystalline appearance and the inorganic counterpart ZrPTE was white granular in nature. The material showed good chemical stability in acidic medium, basic medium and in various organic solvents without any change in nature and appearance. The ion exchange capacity of POT ZrPTE was  $1.45\text{meqg}^{-1}$  whereas the inorganic part showed only a much less value of  $0.63\text{meqg}^{-1}$ .

### 3.2. Material characterization

#### 3.2.1. FT-IR analysis

The FT-IR spectrum of the inorganic component ZrPTE and its poly-o-toluidine composite POT ZrPTE were taken by KBr pellet method. The spectrum bands clearly indicate the formation of ZrPTE and its composite with poly-o-toluidine (Fig. 1). Fig. 1(a) is the IR spectrum of ZrPTE in which the bands at lower frequency ranging from  $500\text{cm}^{-1}$  to  $800\text{cm}^{-1}$  is contributed by metal-oxygen bonding viz: Zr-O and Te-O [24]. The peak observed at  $1052\text{cm}^{-1}$  is the phosphate group stretching frequency [25]. A strong peak at  $1671\text{cm}^{-1}$  is due to the presence of interstitial water molecule in the material. The broad band near  $3402\text{cm}^{-1}$  can be assigned to the characteristic O-H stretching frequency [26]. Fig. 1(b) gives the IR spectrum of POT ZrPTE in which the formation of the composite can be justified by the sharp peak at  $1381\text{cm}^{-1}$  due to the  $\text{sp}^3$  C-H bend and an additional peak at  $3210\text{cm}^{-1}$  which indicates the N-H stretching frequency [25].

#### 3.2.2. TG analysis

The TG analysis of both ZrPTE and POT ZrPTE were carried out in order to compare the thermal stability of the materials. Fig. 2 gives the thermogram comparison of these materials. At around 100 C an initial weight loss of about 10% and 15% takes place in composite and inorganic part respectively, which may be due to the loss of water molecules. From the data, it is clear that ZrPTE withstands major mass loss till around 580 C after which a 5% loss is observed which can be due to any change of phase in the material. With further increase in temperature gradual weight loss was observed and almost 68% weight was retained when the temperature reached 900 °C.

**Table 1**

Synthesis conditions of various samples of POT ZrPTE composite exchanger.

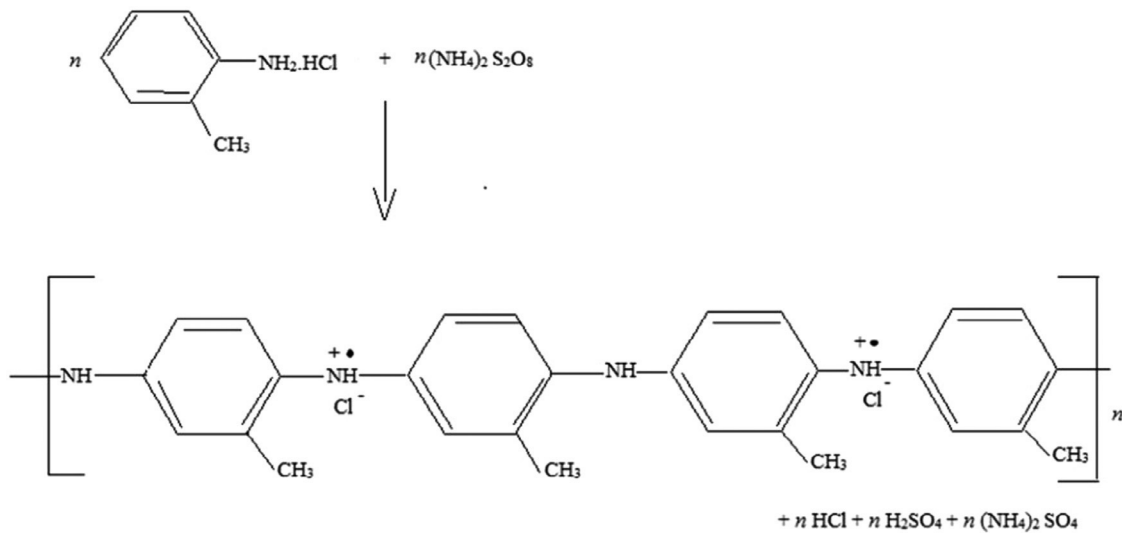
Samples	Mixing volume ratio				pH	Temperature	Appearance	Na <sup>+</sup> IEC ( $\text{meqg}^{-1}$ )
	A	B	C	D				
ZrPTE-1	1	1	1	–	1	25 ± 2 C	White powder	0.53
ZrPTE-2	1	2	1	–	1	25 ± 2 C	White powder	0.48
ZrPTE-3	2	1	1	–	1	25 ± 2 C	White granular	0.59
ZrPTE-4	1	1	2	–	1	25 ± 2 C	White granular	0.63
POT ZrPTE-1	1	1	1	1	1	25 ± 2 C	Green powder	1.1
POT ZrPTE-2	1	2	1	1	1	25 ± 2 C	Dark green powder	0.97
POT ZrPTE-3	2	1	1	1	1	25 ± 2 C	Black granular	1.26
POT ZrPTE-4	1	1	2	1	1	25 ± 2 C	Black granular	1.45

A – 0.05M  $\text{ZrOCl}_2 \cdot 8\text{H}_2\text{O}$  in DMW.

B – 0.05M  $\text{Na}_2\text{HPO}_4$  in DMW.

C – 0.05M  $\text{Na}_2\text{TeO}_3$  in DMW.

D – poly-o-toluidine.



**Scheme 1.** Synthesis of poly-o-toluidine.

For POT ZrPTe, a much rapid loss in weight was observed after 100 °C which may be due to the decomposition of organic part in the composite. At 900 °C, less than 65% weight of POT ZrPTe was retained which indicates that the inorganic part has better thermal stability than the composite. This may be because of the high polymer content in the material.

### 3.2.3. X-ray diffraction study

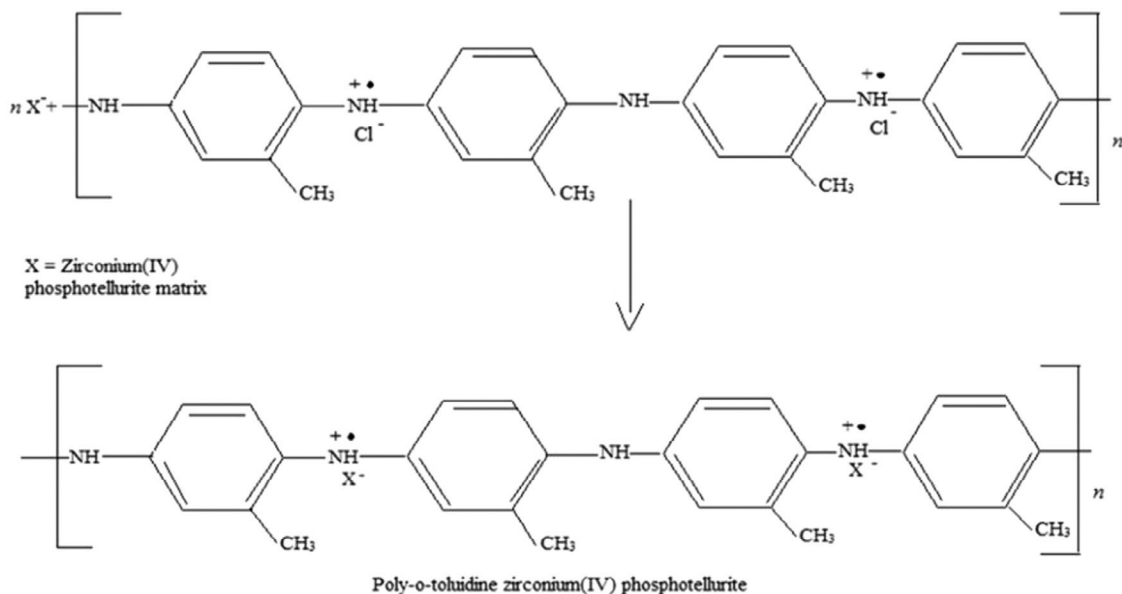
X-ray powder diffraction study was carried out for ZrPTe and POT ZrPTe and the XRD data are shown in Fig. 3. The data reveal that ZrPTe (Fig. 3(a)) is amorphous in nature with broad peaks whereas POT ZrPTe (Fig. 3(b)) displayed highly intense sharp peaks exhibiting the polycrystalline nature of the material. The planes (111) and (210) corresponding to  $2\theta$  values 28.26° and 27.06° correspond to the planes of Te [27,28]. Other major planes (221) and

(330) corresponding to  $2\theta$  values 36.74° and 55.36° can be ascribed to that of Zr and P [29].

### 3.2.4. SEM and EDX analysis

In order to explore the surface morphology of the materials, SEM analysis was carried out. SEM images of ZrPTe and POT ZrPTe (Fig. 4 (a) & (b)) showed drastic difference indicating the morphological change happened after the addition of polymer to the inorganic part. The surface of ZrPTe (Fig. 4(a)) was irregular in nature with scattered appearance. The composite material POT ZrPTe (Fig. 4(b)) showed better surface morphology with uniform surface.

The EDX analysis of POT ZrPTe (Fig. 4(c)) confirmed the formation of composite with the presence of elements Zr, P and Te. The histogram was free of any kind of impurity.



**Scheme 2.** Synthesis of poly-o-toluidine zirconium(IV) phosphotellurite.

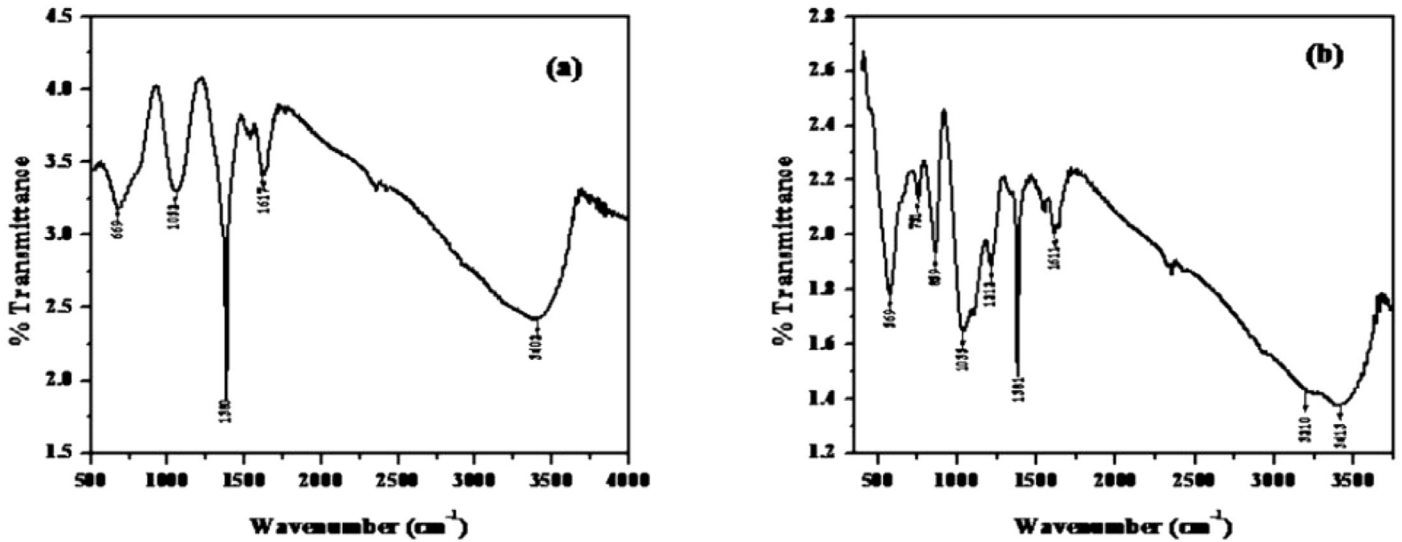


Fig. 1. IR spectrum of (a) ZrPTe and (b) POT ZrPTe.

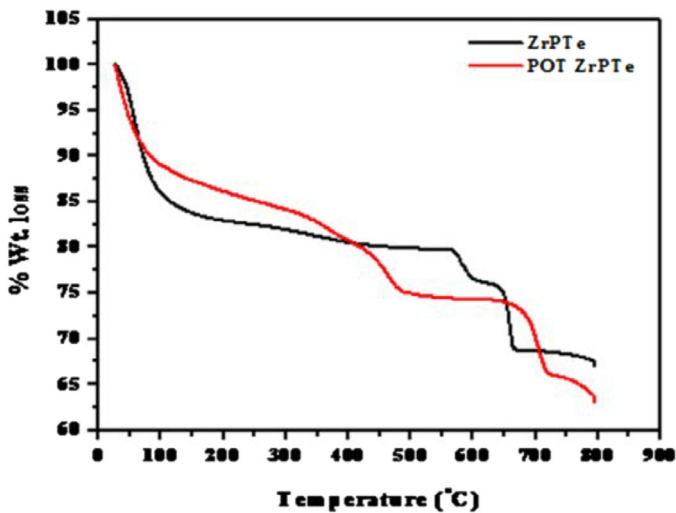


Fig. 2. TG data comparison of ZrPTe and POT ZrPTe.

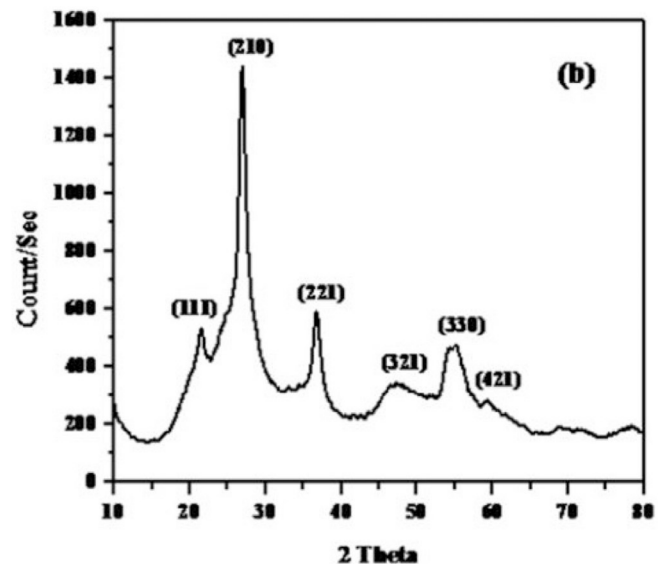
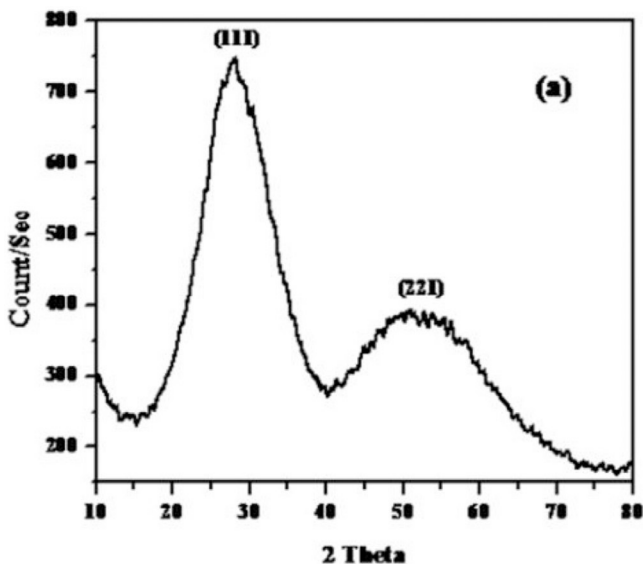


Fig. 3. XRD of (a) ZrPTe and (b) POT ZrPTe.

3.2.5. TEM analysis and colour mapping

The TEM data (Fig. 5 (a)) of POT ZrPTe was taken to find out the particle size of the composite. The TEM image confirmed the nano size (100 nm) of the composite and hence the material can be categorized as nanocomposite. The corresponding colour mapping (Fig. 5(b-d)) of elements Zr, P and Te clearly reveals that the elements are homogeneously dispersed on the polymeric matrix.

3.3. Distribution coefficient study

Distribution coefficient  $K_d$  denotes the selectivity of the material towards a particular ion. The  $K_d$  value of POT ZrPTe towards some heavy metal ions in DMW was studied. POT ZrPTe showed excellent affinity towards Hg(II) ions which can be attributed to its high ion exchange capacity and improved morphology. Table 2 illustrates the  $K_d$  value of POT ZrPTe towards various heavy metal ions.

The  $K_d$  values indicate that it is possible to carry out the sorption of Hg(II) ions from effluents containing mercury. When the  $K_d$  value difference between two metal ions are large, it is possible to separate those metal ions from a solution. Greater the separation factor the easier will be the separation [30]. In this case, since the

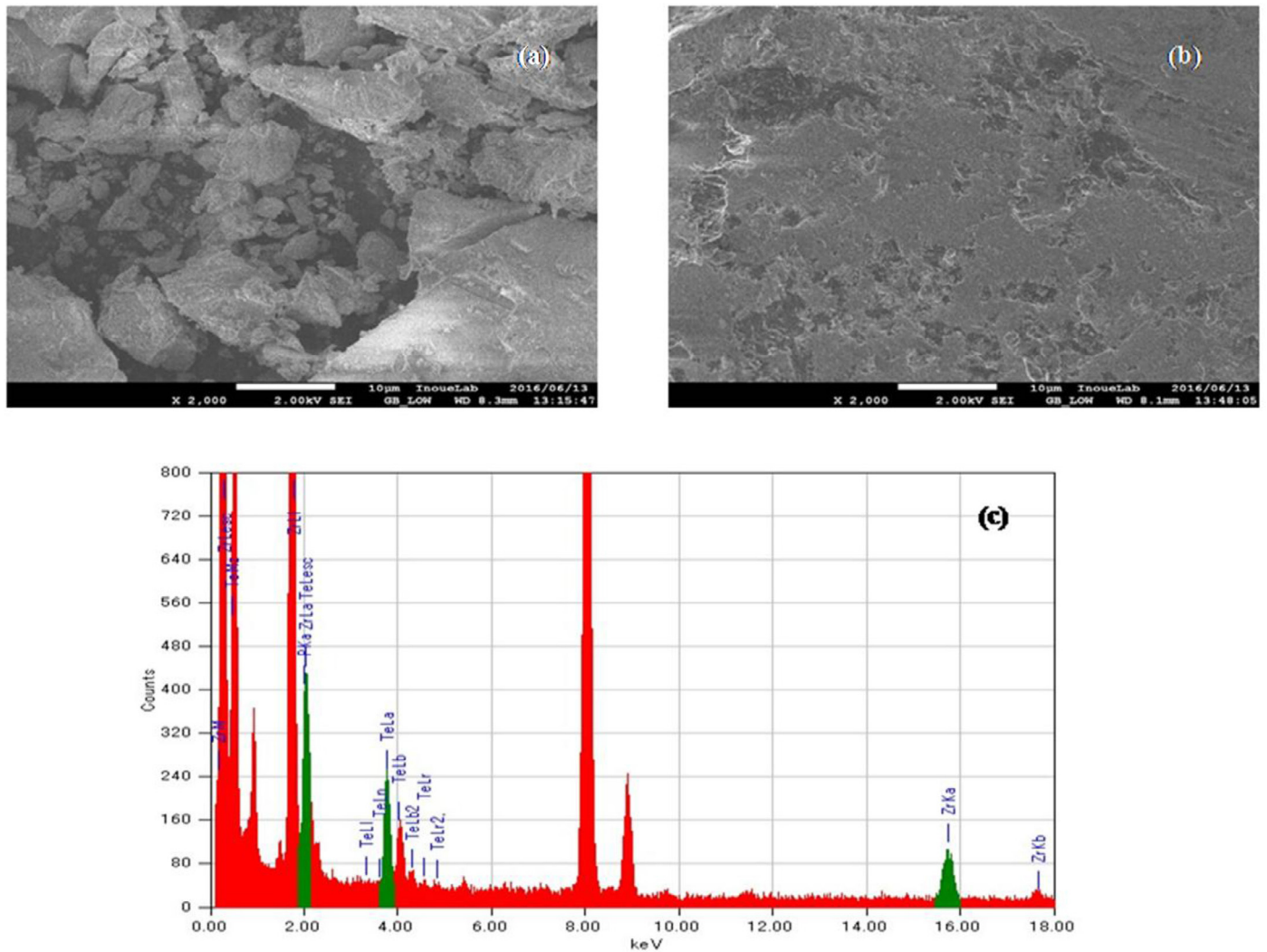


Fig. 4. SEM images of (a) ZrPTE and (b) POT ZrPTE and (c) EDX of POT ZrPTE.

separation factor between the various metal ions are high, binary separation of metal ions are thus possible, which is also an important analytical application.

#### 3.4. Binary separation and quantitative removal of mercury ions

Quantitative separation of metal ions Pb(II), Bi(III), Ni(II) and Th(IV) from synthetic binary mixtures were carried out using the

exchanger (Table 3). Column method was employed for the binary separation. Metal ions which have least affinity towards the exchanger get eluted first followed by the strongly bound ones. Along with the separation of metal ions from synthetic mixtures, quantitative separation of Hg(II) ions from real samples were also carried out using the exchanger. For this, waste water containing Hg(II) from wood industry effluents were collected. The samples were filtered, neutralized and were chemically treated to analyze the

**Table 2**  
Distribution coefficients in water and other electrolytes.

Metal ions	Distribution coefficient ( $K_d$ )						
	DMW	HNO <sub>3</sub>			NH <sub>4</sub> NO <sub>3</sub>		
		0.001M	0.01M	0.1M	0.001M	0.01M	0.1M
Hg(II)	336	57.6	50.8	42	310	53.5	47.6
Cu(II)	125	15.6	3.0	NS	113	9.4	3.1
Pb(II)	106	84.2	76.3	61.2	97.7	80.6	77.0
Bi(III)	100	92	88.3	80.5	94	80.8	62.9
Co(II)	52	38.7	21.5	10	50.2	46.4	16
h(IV)	38	24	13	11	32.7	15	8
Ni(II)	30	12	9	NS	27	10	NS
Zn(II)	17	10	NS	NS	15.3	9	NS
Cd(II)	NS	NS	NS	NS	NS	NS	NS

NS, no observable sorption.

**Table 3**  
Binary separation of metal ions on POT ZrPTE.

Separations achieved	Eluent	Metal ion (mg)		Efficiency %
		Loaded	Eluted	
Hg(II)	1M HNO <sub>3</sub> + 0.1M NH <sub>4</sub> NO <sub>3</sub>	5.13	5.01	97.66
Pb(II)	0.1M HNO <sub>3</sub> + 0.1M NH <sub>4</sub> NO <sub>3</sub>	2.38	2.01	84.55
Hg(II)	1M HNO <sub>3</sub> + 0.1M NH <sub>4</sub> NO <sub>3</sub>	5.05	4.98	98.61
Bi(III)	1.0M HNO <sub>3</sub> + 0.1M NH <sub>4</sub> NO <sub>3</sub>	2.11	2.05	97.15
Hg(II)	1M HNO <sub>3</sub> + 0.1M NH <sub>4</sub> NO <sub>3</sub>	5.67	5.38	94.88
Ni(II)	0.2M HNO <sub>3</sub> + 0.1M NH <sub>4</sub> NO <sub>3</sub>	1.97	1.78	90.35
Hg(II)	1M HNO <sub>3</sub> + 0.1M NH <sub>4</sub> NO <sub>3</sub>	5.58	5.44	97.49
Th(IV)	0.05M HNO <sub>3</sub> + 0.1M NH <sub>4</sub> NO <sub>3</sub>	2.23	2.11	94.61

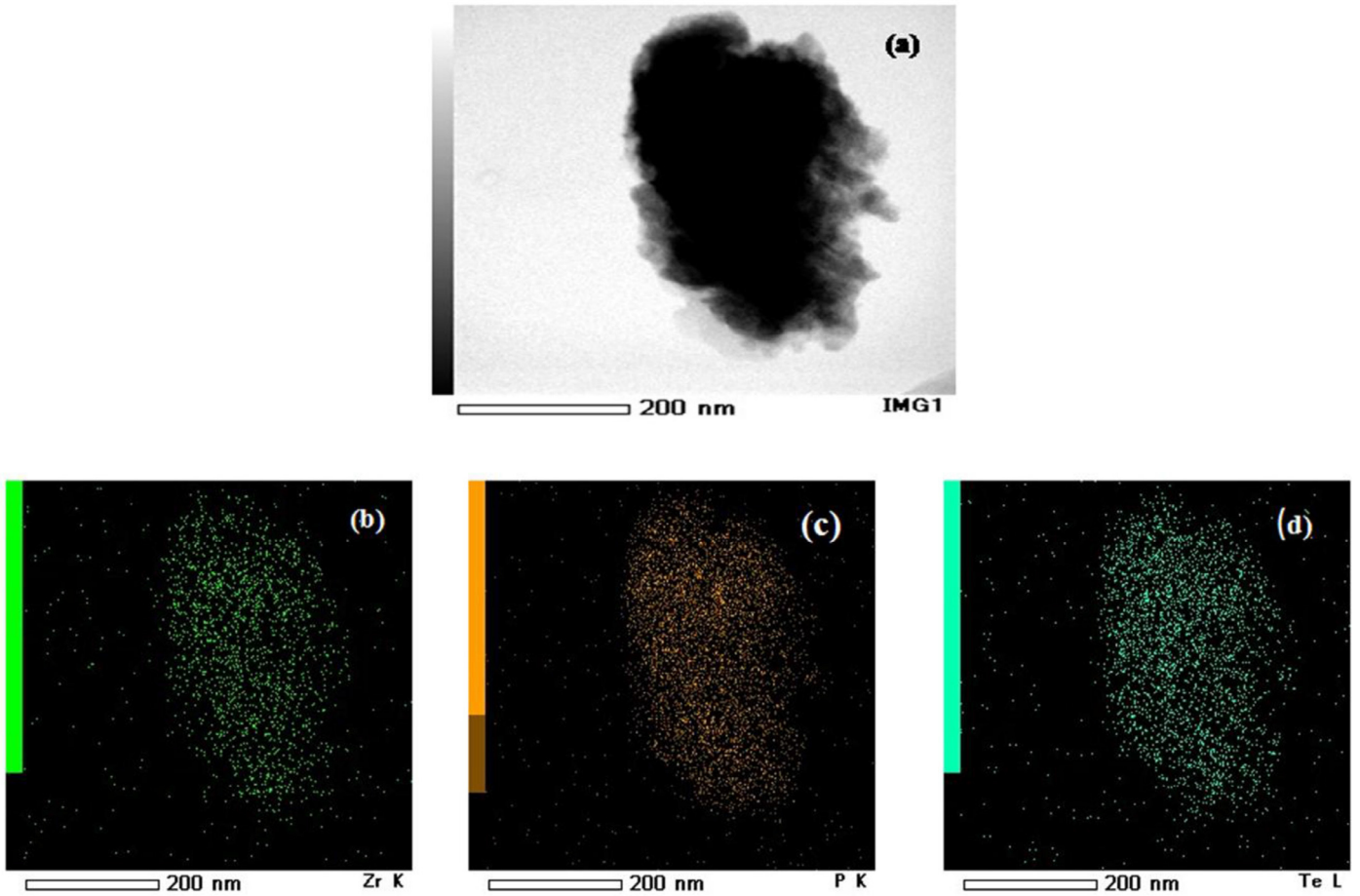


Fig. 5. TEM image of (a) POT ZrPTe; elemental colour mapping of (b) Zr (c) P and (d) Te.

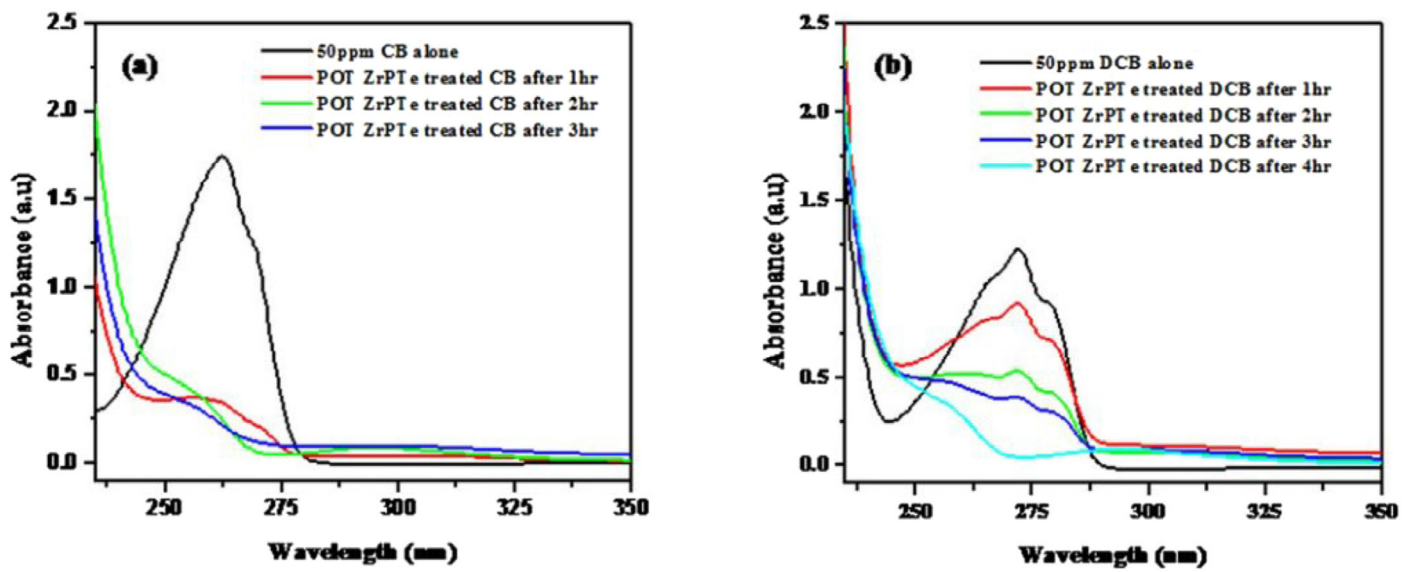


Fig. 6. Equilibrium time UV plot of (a) CB and (b) DCB.

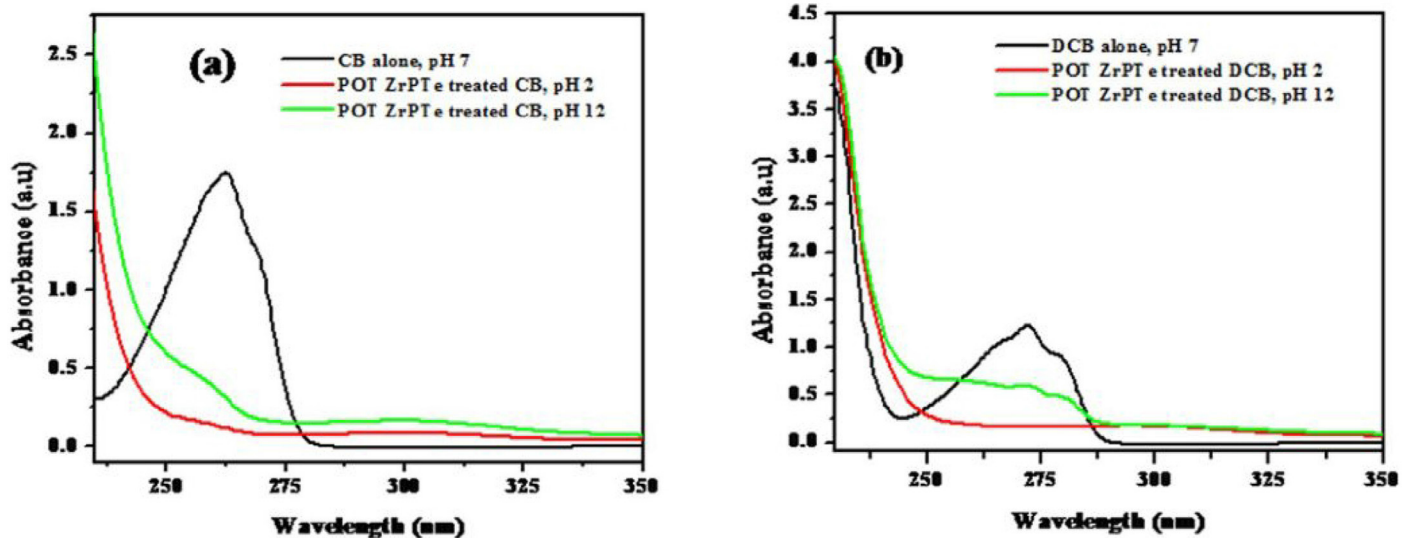


Fig. 7. UV spectra of (a) CB and (b) DCB at different pH range.

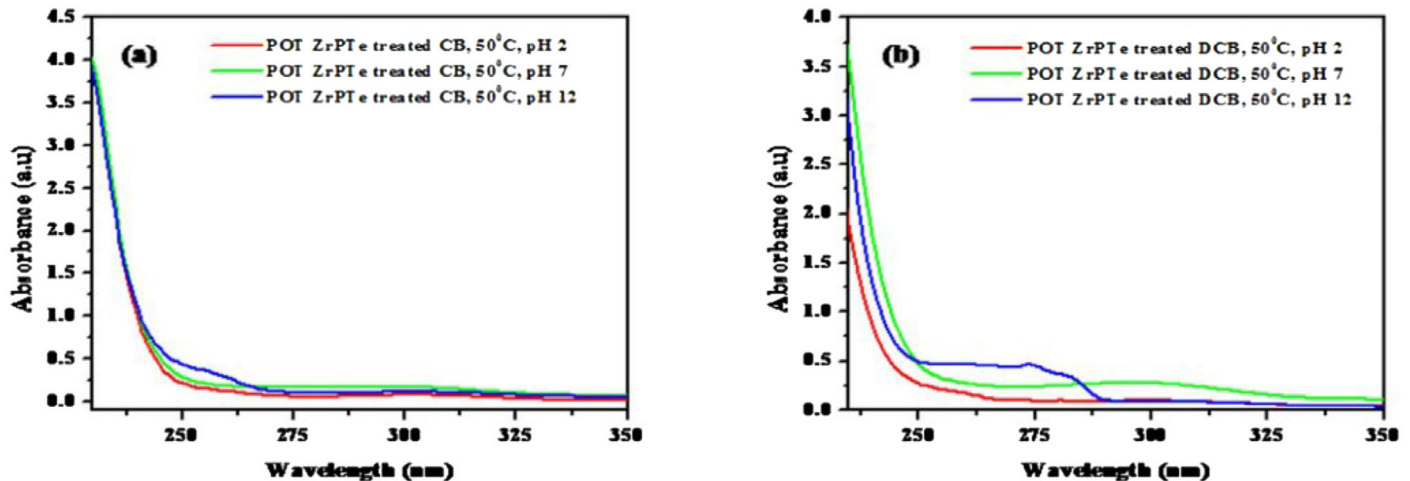


Fig. 8. UV spectra of (a) CB and (b) DCB at 50 C for pH 2, 7 and 12.

Table 4

Quantitative removal of Hg(II) from wood industry effluents.

Sample	Metal ion	Eluent used	In mg/100 mL
Wood industry wastewater (I)	Hg(II)	0.5M HNO <sub>3</sub>	0.95
Wood industry wastewater (II)	Hg(II)	0.5M HNO <sub>3</sub>	0.89

metal ions present in it. 100 mL of the sample was then allowed to pass through the column, enabling the exchange to take place and was collected at the bottom. The experiment was repeated 3–4 times and the flow rate was restricted to 0.5 mL/minute. For eluting out Hg(II) ions, 0.5M HNO<sub>3</sub> was used and the concentration of Hg(II) ions were found out by titration using EDTA solution. 0.95 mg and 0.89 mg of mercury were eluted from 100 mL samples of wood industry effluents using POT ZrPTE (Table 4).

### 3.5. Priority pollutant removal study

The supreme application of POT ZrPTE is its capacity to eliminate priority pollutants like chlorobenzene (CB) and 1,4-dichlorobenzene (DCB). The material successfully removed about 93% of CB and 96% of DCB from aqueous solution. The equilibrium time for maximum adsorption was studied for both CB and DCB. After obtaining the equilibrium time for adsorption, the effects of pH and temperature on adsorption were studied by shaking the pollutants with known amount of POT ZrPTE. The change in concentration of the pollutants can be obtained by measuring their absorbance at  $\lambda_{\max}$  262 nm for CB and 272 nm for DCB using UV spectrophotometer. Since absorbance is directly proportional to concentration of the solution, the percentage of pollutant adsorbed can be calculated using the simple relation,

$$\text{Uptake}(\%) = (C_i - C_f)/C_i \times 100$$

where  $C_i$  and  $C_f$  are the concentration of pollutants before and after adsorption in ppm [31].



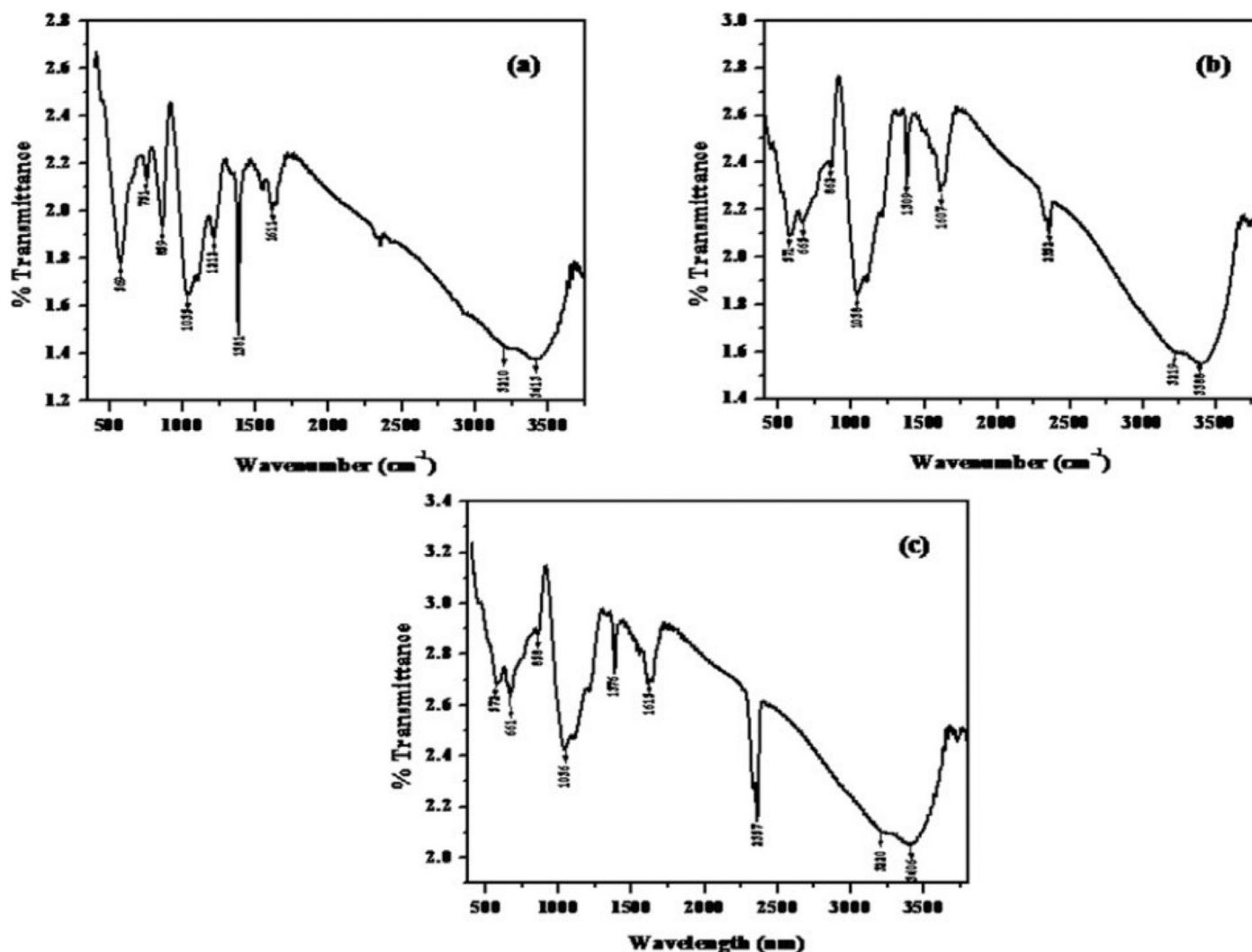


Fig. 9. FT-IR spectra of (a) POT ZrPTe (b) POT ZrPTe\_CB (c) POT ZrPTe\_DCB.

### 3.5.1. Equilibrium time

20 mL of 50 ppm solutions of CB and DCB were shaken in separate beakers with 0.2g of POT ZrPTe at room temperature, till equilibrium state was reached. The rate of adsorption was evaluated by recording the absorbance of the solutions after every hour. Fig. 6 gives the equilibrium time UV plot of CB and DCB at room temperature.

About 79.3% of CB got adsorbed within 1 hour and the adsorption percentage decreased gradually with time (Fig. 6(a)). The high rate of adsorption during the initial stage can be due to the availability of vacant sites on the material. Equilibrium time was achieved within 3 hours and 88% of CB got adsorbed by POT ZrPTe, after which no considerable adsorption was observed. Hence for CB, 3 hours was chosen as the equilibrium time for carrying out further studies. For DCB, around 56.2% got adsorbed within first two hours and the equilibrium was attained after 4 hours (Fig. 6(b)). The maximum uptake percentage after 4 hours was 92% for DCB and the study of all other parameters were carried out by treating DCB with POT ZrPTe for 4 hours.

### 3.5.2. Effect of pH

pH is an important parameter which determines the rate of adsorption. In order to study the pH effect, 0.2g of POT ZrPTe was

shaken with 50 ppm solution of CB and DCB at different pH starting from 2 to 12 at room temperature. For both CB and DCB, maximum adsorption was observed at acidic pH rather than basic pH. Fig. 7 demonstrates the UV spectra of CB and DCB at pH 2, 7 and 12. For both CB and DCB, maximum adsorption was observed at pH 2 and minimum adsorption at pH 12. Almost 92.7% of CB got adsorbed at pH 2 on treatment with POT ZrPTe for 3 hours, whereas only 81% got adsorbed at pH 12 (Fig. 7(a)).

In case of DCB (Fig. 7(b)), 94% got removed at pH 2 when treated with POT ZrPTe for 4 hours but at basic pH, the adsorption percent was as low as 55%. Hence it can be concluded that the adsorption is favored in acidic pH rather than basic pH.

### 3.5.3. Effect of temperature

To study the effect of temperature, the pollutants were equilibrated with 0.2g of POT ZrPTe at 50°C at different pH range. The observations are shown in Fig. 8 and it is clear from the UV spectra that the rate of adsorption increases with increase in temperature. 93% removal was achieved for CB at pH 2 when it was treated with POT ZrPTe for 3 hours. For pH range 7 and 12, the percentage removal was 90.5% and 84% respectively (Fig. 8(a)).

DCB also showed a similar trend of adsorption when temperature was increased. An appreciable removal percentage of 96% was

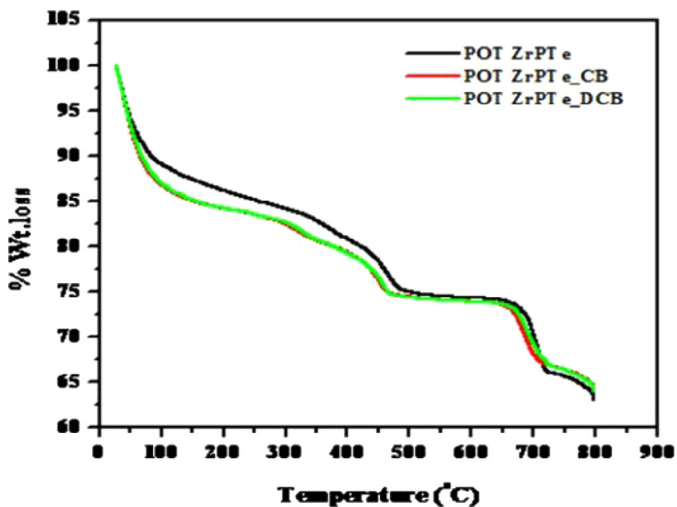


Fig. 10. Thermograms of POT ZrPTe, POT ZrPTe\_CB and POT ZrPTe\_DCB.

achieved when DCB was treated with POT ZrPTe at pH 2 for 4 hours. Comparatively low rate of adsorption of 82% and 63% was observed at pH 7 and 12 respectively at 50 C (Fig. 8(b)).

The adsorption of CB and DCB on to the hybrid exchanger was further confirmed by recording the FT-IR of POT ZrPTe after adsorption of the pollutants. The presence of C-Cl bonding gives IR peak in the range  $660\text{ cm}^{-1}$  [32]. The IR spectrum of POT ZrPTe after adsorption clearly exhibited additional peaks corresponding to C-Cl stretching frequency at  $665\text{ cm}^{-1}$  and  $661\text{ cm}^{-1}$  for POT ZrPTe\_CB and POT ZrPTe\_DCB. The FT-IR data of POT ZrPTe before and after adsorption of CB and DCB is shown in Fig. 9.

As an extension study, the thermal stability of POT ZrPTe was examined after pollutant adsorption. The TG analysis was carried out to check whether any kind of thermal instability occurred to the material after adsorption of the pollutants. The thermogram of POT ZrPTe after adsorption is given in Fig. 10 which clearly indicates that no thermal instability has occurred after the adsorption of pollutants since the thermogram of POT ZrPTe, POT ZrPTe\_CB and POT ZrPTe\_DCB showed almost similar degradation pattern.

Table 5

Parameters of adsorption of chlorobenzene for pseudo-first order and pseudo-second order kinetics models.

Pseudo-first order			Pseudo-second order		
$q_e$ (mg/g)	$K_1$ ( $\text{min}^{-1}$ )	$R^2$	$q_e$ (mg/g)	$K_2$ (g/mgmin)	$R^2$
4.08804	0.0178	0.9805	9.3283	0.0107	0.9976

Only a slight change in the weight loss of about 4% was observed in POT ZrPTe after adsorption.

### 3.6. Kinetic studies

The adsorption kinetics of CB and DCB on to POT ZrPTe was analyzed by pseudo-first order and pseudo-second order kinetic models. The rate constant  $k_1$  for pseudo-first order was studied using the Lagergren rate equation [33] and pseudo-second-order equation given by Ho and McKay was used for the obtaining the rate constant  $k_2$  [34].

Pseudo-first-order:

$$\log(q_e - q_t) = \log q_e - k_1 t / 2.303$$

Pseudo-second-order:

$$\frac{t}{q_t} = \frac{1}{k_2 q_e^2} + \frac{t}{q_e}$$

where  $q_e$  and  $q_t$  are the adsorption capacities at equilibrium at time  $t$ ;  $k_1$  and  $k_2$  are pseudo-first-order and pseudo-second-order rate constants respectively.  $k_1$  can be determined from the slope of the plot  $\log(q_e - q_t)$  versus  $t$  and  $k_2$  from the intercepts of the plot  $t/q_t$  versus  $t$ .

Fig. 11(a) and (b) is the linear plot of pseudo first order model of CB and DCB onto POT ZrPTe, and Fig. 12(a) and (b) is the pseudo second order model of CB and DCB onto POT ZrPTe. The kinetic parameters calculated from the plots are given in Tables 5 and 6. The comparison of  $R^2$  value in both cases suggests that the pseudo second order is the more suitable model for adsorption which indicates that the nature of adsorption is chemisorption [34].

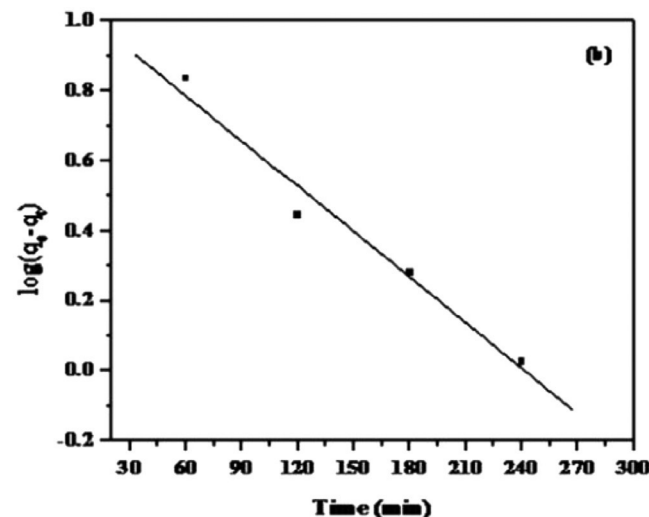
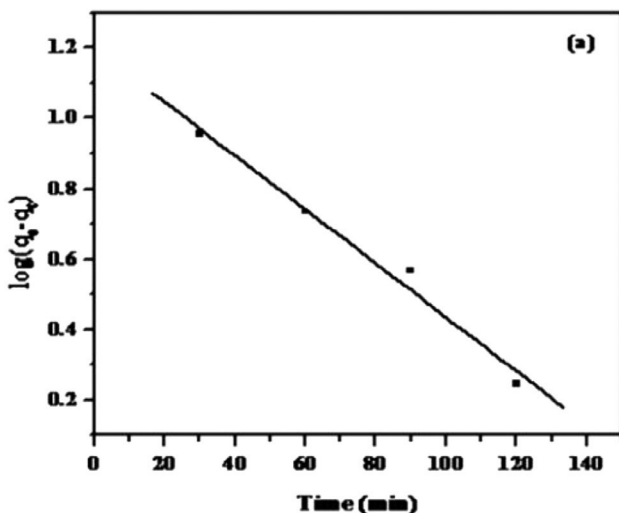


Fig. 11. Linear plots of pseudo-first order kinetic model of (a) POT ZrPTe\_CB and (b) POT ZrPTe\_DCB.

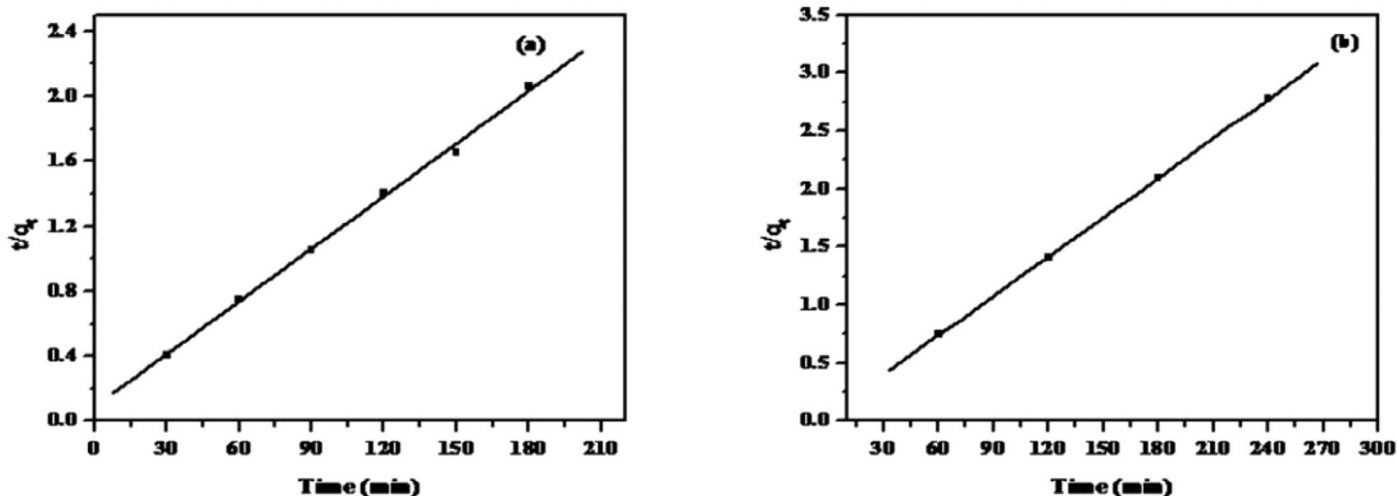


Fig. 12. Linear plots of pseudo-second order kinetic model of (a) POT ZrPte\_CB and (b) POT ZrPte\_DCB.

Table 6

Parameters of adsorption of 1,4-dichlorobenzene for pseudo-first order and pseudo-second order kinetics models.

Pseudo-first order			Pseudo-second order		
$q_e$ (mg/g)	$K_1$ ( $\text{min}^{-1}$ )	$R^2$	$q_e$ (mg/g)	$K_2$ (g/mgmin)	$R^2$
5.0118	0.0092	0.9730	14.5524	0.0368	0.9998

#### 4. Conclusion

The nanocomposite exchanger poly-o-toluidine zirconium(IV) phosphotellurite was synthesized by simple sol gel method. The material was stable in various solvents and showed better ion exchange capacity than its inorganic counterpart. It was characterized using different instrumental techniques like FT-IR, TGA, XRD, SEM-EDX and TEM. The composite exchanger displayed good selectivity towards Hg(II) ions. Binary separation of metal ions from synthetic mixtures and waste water treatment of wood industry effluent containing Hg(II) ions were also carried out. The main application of the material was its ability to adsorb organic priority pollutants like chlorobenzene and 1,4-dichlorobenzene from aqueous solution. Different parameters which affect the rate of adsorption like time, pH and temperature were studied and the material could successfully remove about 93% of CB and 96% of DCB at pH 2. It took about 3 hours for maximum adsorption of CB and about 4 hours for DCB. The material retained its thermal stability even after the adsorption of the pollutants. The kinetic aspects of adsorption were also studied in detail. Kinetic parameters suggest that pseudo second order model is the more suitable kinetic model. The results clearly validate that the material POT ZrPte is an excellent agent for salvation of environment from pollutants.

#### Acknowledgement

Author Aparna Mohan, acknowledges the Council of Scientific and Industrial Research for awarding Junior Research Fellowship. The technical support provided by the Department of Applied Chemistry, Tokyo Metropolitan University, Japan, is also gratefully acknowledged.

#### References

- [1] A.Z.M. Badruddoz, Z.B.Z. Shawon, T.W.J. Daniel, K. Hidajat, M. Shahabuddin,  $\text{Fe}_3\text{O}_4$ /cyclodextrin polymer nanocomposites for selective heavy metals removal from industrial wastewater, *Carbohydr. Polym* 91 (2013) 322–332.
- [2] Z.A. Al-Othman, M. Naushad, Inamuddin, Organic-inorganic type composite cation exchanger poly-o-toluidine Zr(IV) tungstate: preparation, physicochemical characterization and its analytical application in separation of heavy metals, *Chem. Eng. J.* 172 (2011) 369–375.
- [3] V.K. Gupta, Suhas, Application of low-cost adsorbents for dye removal—a review, *J. Environ. Manag* 90 (2009) 2313–2342.
- [4] M. Xu, Y. Zhang, Z. Zhang, Y. Shen, M. Zhao, G. Pan, Study on the adsorption of  $\text{Ca}^{2+}$ ,  $\text{Cd}^{2+}$  and  $\text{Pb}^{2+}$  by magnetic  $\text{Fe}_3\text{O}_4$  yeast treated with EDTA dianhydride, *Chem. Eng. J.* 168 (2011) 737–745.
- [5] H. Cesur, N. Balkay, Zinc removal from aqueous solution using an industrial by-product phosphogypsum, *Chem. Eng. J.* 131 (2007) 203–208.
- [6] United States Environmental Protection Agency, Toxic and priority pollutants under the clean water act, 2000. Washington, D.C.: Office of Environmental Information <https://www.epa.gov/eg/toxic-and-priority-pollutants-under-clean-water-act>.
- [7] A. Khan, A.M. Asiri, M.A. Rub, N. Azum, A.A.P. Khan, I. Khan, et al., Review on composite cation exchanger as interdisciplinary materials in analytical chemistry, *Int. J. Electrochem. Sci* 7 (2012) 3854–3902.
- [8] N. Mu, Inorganic and composite ion exchange materials and their applications, *Ion Ex. Lett* 2 (2009) 1–14.
- [9] D.A. Clifford, Ion Exchange and Inorganic Adsorption, *Water Quality and Treatment: A Handbook of Community Water Supplies*, fifth ed., McGraw-Hill, 1999.
- [10] M.A. Barakat, New trends in removing heavy metals from industrial wastewater, *Arab. J. Chem* 4 (2011) 361–377.
- [11] S.A. Nabi, M. Shahadat, R. Bushra, A.H. Shalla, Heavy-metals separation from industrial effluent, natural water as well as from synthetic mixture using synthesized novel composite adsorbent, *Chem. Eng. J.* 175 (2011) 8–16.
- [12] F. Fua, Q. Wang, Removal of heavy metal ions from wastewaters: a review, *J. Environ. Manage* 92 (2011) 407–418.
- [13] Y. Guo, Y. Li, T. Zhu, M. Ye, X. Wang, Adsorption of  $\text{SO}_2$  and chlorobenzene on activated carbon, *Adsorption* 19 (2013) 1109–1116.
- [14] L.D. Asnin, V.A. Davankov, A.V. Pastukhov, The adsorption of chlorobenzene on a carbon adsorbent obtained by the pyrolysis of hypercrosslinked polystyrene, *Russ. J. Phys. Chem. A* 82 (2008) 2313–2317.
- [15] K. Balamurugan, V. Subramanian, Adsorption of chlorobenzene onto (5,5) armchair single-walled carbon nanotube and graphene sheet: toxicity versus adsorption strength, *J. Phys. Chem. C* 117 (2013) 21217–21227.
- [16] X.-K. Zhao, G.-P. Yang, P. Wu, N.-H. Li, Study on adsorption of chlorobenzene on marine sediment, *J. Colloid Interface Sci* 243 (2001) 273–279.
- [17] L.D. Asnin, A.A. FedorovYu, S. Chekryshkin, Adsorption of chlorobenzene and benzene on  $\gamma\text{-Al}_2\text{O}_3$ , *Russ. Chem. Bull* 50 (2001) 68–72.
- [18] Q. Liu, Y. Chen, J. Wang, J. Yu, J. Chen, G. Zhou, Electrochemical oxidation of 1,4-dichlorobenzene on platinum electrodes in acetonitrile-water solution: evidence for direct and indirect electrochemical oxidation pathways, *Int. J. Electrochem. Sci* 6 (2011) 2366–2384.
- [19] X.-G. Li, M.-R. Hung, R. Liu, Facile synthesis of semi-conducting particles of oxidative melamine/toluidine copolymers with solvatochromism, *React. Funct. Polym* 62 (2005) 285–294.
- [20] A. Vogel, *A Textbook of Practical Organic Chemistry*, Longman Group Limited, London, 1975.
- [21] C.E. Harland, *Ion Exchange: Theory and Practice*, RSC, 1994.
- [22] M. Marhol, *Ion Exchangers in Analytical Chemistry: Their Properties and Use in Inorganic Chemistry*, Academia, Prague, 1982.
- [23] W.F. Forbes, Light absorption studies: the ultraviolet absorption spectra of chlorobenzenes, *Can. J. Chem* 38 (1960) 1104–1112.
- [24] C.N.R. Rao, *Chemical Applications of Infrared Spectroscopy*, Academic Press, New York, 1963.

- [25] C. Sandorfy, T. Theophanides, *Spectroscopy of Biological Molecules: Theory and Applications*, Springer, New York, 1984.
- [26] A.A. Khan, S. Shaheen, Synthesis and characterization of a novel hybrid nano composite cation exchanger poly-o-toluidine Sn(IV) tungstate: its analytical applications as ion-selective electrode, *Solid State Sci* 16 (2013) 158–167.
- [27] M.K. Trivedi, R.M. Tallapragada, A. Branton, D. Trivedi, G. Nayak, O.P. Latiyal, et al., Evaluation of atomic, physical and thermal properties of tellurium powder: impact of biofield energy treatment, *J. Electr. Electron. Syst* 4 (2015) 3.
- [28] V.D. Novruzov, N.M. Fathi, O. Gorur, M. Tomakin, A.I. Bayramov, S. Schorr, et al., CdTe thin film solar cells prepared by a low-temperature deposition method, *Phys. Status Solidi A*. 207 (2010) 730–733.
- [29] P.B. Moore, T. Araki, I.M. Steele, G.H. Swihart, A.R. Kampf, Gainesite, sodium zirconium beryllophosphate: a new mineral and its crystal structure, *Am. Mineral* 68 (1983) 1022–1028.
- [30] F.G. Helfferich, *Ion Exchange*, McGraw-Hill, 1962.
- [31] S. Mondal, Methods of dye removal from dye house effluent-an overview, *Environ. Eng. Sci* 25 (2008) 383–396.
- [32] V. Kumar, Y. Panickar, M.A. Palafox, J.K. Vats, I. Kostova, K. Lang, et al., Ab-initio calculations, FT-IR and FT Raman spectra of 2-chloro-6-methyl benzonitrile, *Indian J. Pure Appl. Phys* 48 (2010) 85–94.
- [33] C. Raji, T.S. Anirudhan, Batch Cr(VI) removal by polyacrylamide grafted sawdust: kinetics and thermodynamics, *Water Res* 32 (1998) 3772–3780.
- [34] Y.S. Ho, G. McKay, Sorption of dye from aqueous solution by peat, *Chem. Eng. J.* 70 (1998) 115–124.